JPE 15-5-27

http://dx.doi.org/10.6113/JPE.2015.15.5.1409
ISSN(Print): 1598-2092 / ISSN(Online): 2093-4718

A Double Bi-Quad Filter with Wide-Band Resonance Suppression for Servo Systems

Xin Luo†, Anwen Shen*, and Renchao Mao*

†*School of Automation, Huazhong University of Science and Technology, Wuhan, China

Abstract

In this paper, an algorithm using two bi-quad filters to suppress the wide-band resonance for PMSM servo systems is proposed. This algorithm is based on the double bi-quad filters structure, so it is named, "double bi-quad filter." The conventional single bi-quad filter method cannot suppress unexpected mechanical terms, which may lead to oscillations on the load side. A double bi-quad filter structure, which can cancel the effects of compliant coupling and suppress wide-band resonance, is realized by inserting a virtual filter after the motor speed output. In practical implementation, the proposed control structure is composed of two bi-quad filters on both the forward and feedback paths of the speed control loop. Both of them collectively complete the wide-band resonance suppression, and the filter on the feedback path can solve the oscillation on the load side. Meanwhile, with this approach, in certain cases, the servo system can be more robust than with the single bi-quad filter method. A step by step design procedure is provided for the proposed algorithm. Finally, its advantages are verified by theoretical analysis and experimental results.

Key words: Bi-quad filter, PMSM servo, Self-adaption, System identification, Wide-band resonance

I. INTRODUCTION

Permanent magnet synchronous motor servo drives are used in a wide range of industrial applications [1]-[4]. A response bandwidth and dynamic stiffness are two key ratings for its performance [5]-[7]. Therefore, the drive must be configured with high gains to achieve high performance. However, if a compliant coupling exists between the motor and the load, the high controller gains may lead to severe mechanical resonance and oscillation.

Researchers have proposed many solutions to suppress mechanical resonance. These include pole placement methods with a PID structure [8]-[10], two degrees of freedom (DOF) robust controllers with a μ-Synthesis architecture [11], [12], additional state feedback methods [13]-[17], detecting the resonant frequency (such as FFT) and designing the Notch filter [18]-[22], oscillation suppression with fuzzy neural network wave controllers [23], [24], etc. Due to their simplicity and short convergence times, notch filters and acceleration feedback are widely used in industry applications at present. However, most research is focused on a specific condition, and cannot be applied in the case of wide-band resonance suppression.

George Ellis divides resonance into two categories: high-frequency resonance and low-frequency resonance [15]. High-frequency resonance can occur only over a narrow range of frequencies and its resonance frequency is close to or higher than the crossover frequency. The machines that suffer the most from this kind resonance are those with stiff mechanical structures and low damping, such as lathes. The notch filter method can achieve a good effect in terms of high-frequency resonance suppression [15]. For the acceleration feedback method, it has less effect on high-frequency resonances suppression because the gain peak at the resonance frequency is usually very high [17], [20].

For low-frequency resonance, it occurs over a wide range of frequencies and its resonance frequency is less than the crossover frequency [15]. Low-frequency resonance often appears when the inertia ratio is large and the transmission component is flexible, such as in laser typesetters. The acceleration feedback method has good performance in terms of low-frequency resonance suppression. However, the notch filter is not effective because it can only reduce amplitude

Manuscript received Jan. 22, 2015; accepted May 5, 2015
Recommended for publication by Associate Editor Dong-Myung Lee.
†Corresponding Author: hust_luox@126.com
Tel: +86-027-8754-1547, Fax: +86-027-8754-1547, Huazhong University of Science and Technology
*School of Automation, Huazhong Univ. of Science and Tech., China

© 2015 KIPE

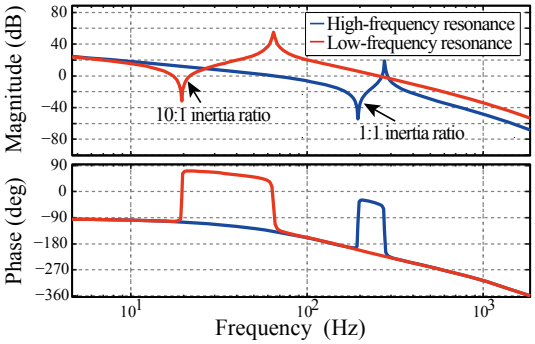

Fig. 1. Mechanical resonance change between high-frequency and low-frequency resonance.

gains in a narrow bandwidth [15].

In some industrial applications such as winding machines and robotic arms, if the spring constant of the connecter is not very high, the mechanical resonance may change between a high and low frequency resonance according to the load inertia and system damping term variations, as shown Fig. 1. In Fig. 1, the category of the resonance is high-frequency resonance when the load-to-inertia ratio is 1:1. With the increasing of the inertia ratio to 10:1, the resonance is changed from high-frequency resonance to low-frequency resonance.

In order to solve these problems, servo systems often require the use of step-by-step engineering solutions. For example, acceleration feedback is used in low-frequency resonance and the notch filter is adopted for high-frequency resonance. However, the switching condition between them is difficult to determine. Therefore, it is necessary to design a scheme for wide-band resonance suppression.

In existing solutions, the bi-quad filter can eliminate the effects of compliant coupling, and correct the motor and load as an ideal rigidly-coupled system [13], [25]. In a sense, the bi-quad filter can be applied to wide-band resonance suppression. However, the bi-quad filter has two shortcomings, which constrain its application. Firstly, the load side may still oscillate after adding a bi-quad filter. Secondly, the filter is very sensitive to system parameters such as load inertia and spring constant [13]. Overall, the single bi-quad filter structure is the main cause of these shortcomings.

Therefore, in order to suppress wide-band resonance, an advanced double bi-quad filter method is proposed in this paper. Its design procedure, robustness analysis and self-adaptive control strategy according to parameter changes are also investigated. Simulation and experimental results show that the proposed structure can be applied for wide bandwidth resonance suppression. The proposed double bi-quad filter can solve the problem of load side oscillation. If the stability margin is reduced by parameter errors but the system is still stable, the proposed structure can alleviate the damage caused by the parameter errors. If a change in the parameters makes the system unstable, parameter modification and reconstruction are necessary for both the single bi-quad filter and the proposed double bi-quad filter.

This paper is arranged as follows. In Section II, the load side oscillation and parameters sensitivity of the single bi-quad filter are analyzed. To solve these problems and to realize wide-band resonance suppression, a double bi-quad filter and its design procedure are proposed in Section III. In order to further improve the proposed double bi-quad filter, parameter sensitivity and a self-adaptive method are analyzed in Section IV. In Section V, experimental results verify the advantages of the proposed double bi-quad filter structure, and conclusions are made in the last section.

II. Disadvantages of the Single Bi-Quad Filter

For two-mass systems, the transfer function from the drive torque, T_e, to the motor speed, ω_m, is:

$$\frac{\omega_{\mathrm{m}}}{T_e} = G_1(\mathrm{s})G_2(\mathrm{s}), G_1(\mathrm{s}) = \frac{1}{(J_m + J_L)s}$$
$$G_2(\mathrm{s}) = \frac{J_L s^2 + K_w s + K_s}{J_p s^2 + K_w s + K_s}, J_p = \frac{J_m J_L}{J_m + J_L} \quad (1)$$

Where, J_m and J_L are the motor and load inertias, respectively. K_s and K_w are the equivalent spring constant and the viscous damping constant, respectively. $G_1(s)$ is a rigidly-coupled transfer function between the motor and the load, and $G_2(s)$ is the effect of the compliant coupling.

$G_2(s)$ causes instability by altering the phase and gain of the lumped inertial plant. The viscous damping, K_w, for most machines is low so that both the numerator and denominator are lightly damped. The un-damped values of the anti-resonant frequency f_{ares} and the resonant frequency f_{res} are:

$$f_{ares} = \frac{1}{2\pi}\sqrt{\frac{K_s}{J_L}}, f_{res} = \frac{1}{2\pi}\sqrt{\frac{K_s}{J_p}} \quad (2)$$

Fig. 2 shows a typical speed control system used in industry. ω_{ref} is the reference speed. $G_{nc}(s)$ is equal to $G_n(s)G_c(s)$. $G_n(s)$ is a PI controller for the speed loop, which contains a proportionality factor, K_n, and an integral time t_n. The models used in this paper rely on a first-order low-pass filter (Equ. (4)) acting as the current loop, which contains a torque coefficient, K_t, a speed detection delay time, T_f, and a current loop equivalent delay time T_{ci}. The motor speed, ω_m, is connected to the mechanical function $G_3(s)$, and the load speed, ω_L, is obtained.

$$G_n(s) = \frac{K_n t_n s + K_n}{t_n s} \quad (3)$$

$$G_c(s) = \frac{K_t}{(T_f + T_{ci})s + 1} \quad (4)$$

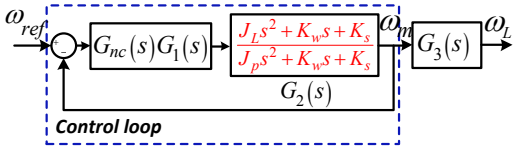

Fig. 2. Industrial speed control system.

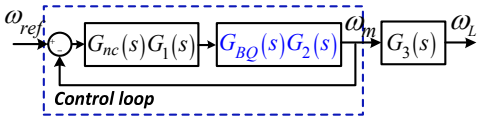

Fig. 3. Industrial speed system with ideal single bi-quad filter.

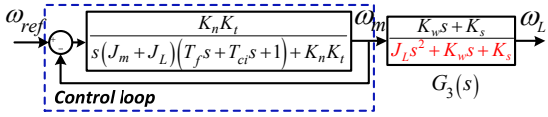

Fig. 4. Simplified single bi-quad filter system.

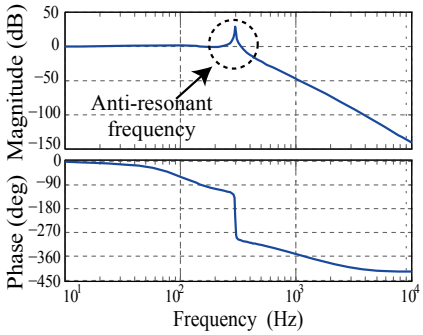

Fig. 5. Bode plot from ω_{ref} to ω_L.

$$G_3(s)=\frac{K_ws+K_s}{J_Ls^2+K_ws+K_s} \tag{5}$$

The single bi-quad filter (conventional bi-quad filter) is designed to cancel the effects of $G_2(s)$. It has the ideal form:

$$G_{BQ}(s)=\frac{J_ps^2+K_ws+K_s}{J_Ls^2+K_ws+K_s} \tag{6}$$

If the ideal form is achieved, the single bi-quad filter may eliminate the effect of $G_2(s)$, leaving $G_1(s)$ as an ideal inertial load as shown in Fig. 3. This will enhance the response speed and dynamic stiffness as much as possible [13].

However, the single bi-quad filter has two major shortcomings. First, the motor speed may be controlled without oscillations. However, the load speed, which is connected to the motor through a compliant coupling, still resonates. The second shortcoming is that the servo system is very sensitive to parameter changes. If the parameters such as load inertia or spring constant are changed, the control loop may become unstable [13].

Fig. 4 shows a simplified single bi-quad filter speed control system. Since the integration only affects the system response characteristics at low frequencies, $G_n(s)$ is simplified as a P-controller. The control loop is corrected as a rigidly-coupled system. This indicates that no oscillations are

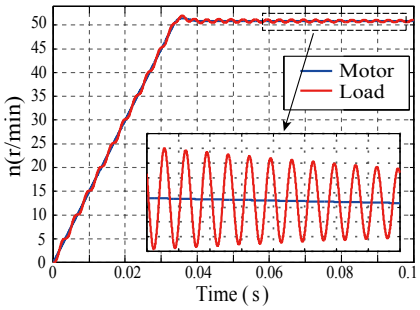

Fig. 6. Motor damping and load oscillation with properly tuned single bi-quad filter.

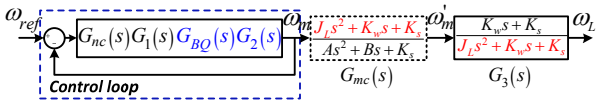

Fig. 7. Single bi-quad filter system with $G_{mc}(s)$.

to be expected on the motor side. However, in the transfer function $G_3(s)$, the term $(J_Ls^2+K_ws+K_s)$ produces a very high gain at the anti-resonant frequency f_{ares}.

The effect of this term is seen in the Bode plot from ω_{ref} to ω_L (Fig. 5), where the gain is maximized at f_{ares}. Consequently, an oscillation is expected on the load side, as shown in Fig. 6.

III. Derivation of the Double Bi-Quad Filter to Achieve a Virtual Mechanical Connector

Theoretically, the single bi-quad filter is designed to eliminate the effects of the compliant coupling. However, it has limitations as mentioned above. To overcome these problems, a double bi-quad filter is proposed in this section.

A. Derivation of the Proposed Double Bi-quad Filter

When a single bi-quad filter is added in the forward path, a load oscillation is caused by the peaking of $1/(J_Ls^2+K_ws+K_s)$ in $G_3(s)$. If the term $(J_Ls^2+K_ws+K_s)$ can be cancelled or replaced, the oscillation on the load side may be suppressed. Consequently, a term $G_{mc}(s)$ is added in front of $G_3(s)$ to weaken the effects of the problem term $(J_Ls^2+K_ws+K_s)$. In order to eliminate this problem term, $G_{mc}(s)$ can be designed as in Fig. 7, where the denominator of $G_3(s)$ is cancelled by the numerator of $G_{mc}(s)$, and is replaced with a new term (As^2+Bs+K_s). In this case, the oscillation of the load can be eliminated by tuning the parameters A and B in $G_{mc}(s)$. The design of A and B is analyzed in next part. Finally, the oscillation on the load side is eliminated.

In Fig. 7, the frames after ω_m are not included in the control loop. The effort of changing $G_{mc}(s)$ to alter $G_3(s)$ is equivalent to redesigning the mechanical coupling. However, this method is not always practical and may increase the cost. Instead, $G_{mc}(s)$ can be realized by adding a digital filter in the control loop.

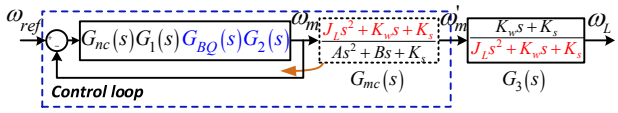

Fig. 8. Move filter $G_{mc}(s)$ into control loop.

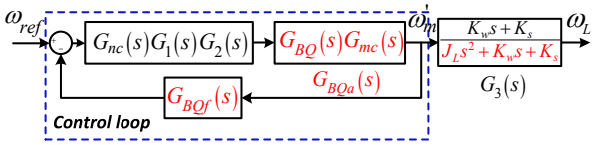

Fig. 9. Industrial speed system with ideal double bi-quad filter.

According to Fig. 7, the low-frequency gain of $G_{mc}(s)$ is 1, which guarantees that $\omega_m = \omega_m'$ in the steady state. As a result, $G_{mc}(s)$ can be included directly into the control loop, which changes the dynamic response of ω_m without a static error as shown in Fig. 8.

Considering the realization of the digital control, the control loop needs to be further modified. The filter $G_{mc}(s)$ can be transferred to the forward and feedback paths of the closed-loop as shown in Fig. 9.

After modifying the system frame, the filter on the forward path is $G_{BQa}(s)=G_{BQ}(s)G_{mc}(s)$ while the filter on the feedback path is $G_{BQf}(s)=G_{mc}^{-1}(s)$. The bi-quad filters on the forward path and the feedback path are given by:

$$\begin{cases} G_{BQa}(s) = \dfrac{J_p s^2 + K_w s + K_s}{As^2 + Bs + C} \\ G_{BQf}(s) = \dfrac{As^2 + Bs + C}{J_L s^2 + K_w s + K_s} \end{cases} \tag{7}$$

The transfer function of the new system's open-loop is:

$$G_{mo}(s) = \frac{K_n K_t}{s\left(T_f s + T_{ci} s + 1\right)\left(J_m + J_L\right)} \tag{8}$$

The transfer function from the speed reference, ω_{ref}, to the load speed, ω_L, is:

$$G_L(s) = \frac{K_n K_t\left(K_w s + K_s\right)}{\left(s\left(J_m + J_L\right)\left(T_f s + T_{ci} s + 1\right) + K_n K_t\right)\left(As^2 + Bs + K_s\right)} \tag{9}$$

$G_{mo}(s)$ shows that the new system's open-loop characteristic is the same as that in the rigidly connected system, while $(J_L s^2+K_w s+K_s)$ in the denominator of $G_L(s)$ is changed to (As^2+Bs+K_s). The suppression of the load side oscillation can be obtained by tuning A and B, which makes $1/(As^2+Bs+K_s)$ a low pass filter without peaking. When compared with the single bi-quad filter scheme, there are two bi-quad filters in the control loop. Therefore, it is called a "double bi-quad filter" in this paper.

B. Design of the Double Bi-Quad Filter

The design of the double bi-quad filter requires several parameters, such as the gains of the speed and current loops, the delay times, T_f and T_{ci}, the spring constant, K_s, the damping constant, K_w, the motor inertia, J_m, the load inertia, J_L, and the filter parameters A and B.

Among them, the PI controllers can be designed on the basis of [31]. In general, mechanical resonance occurs in high controller gains which can achieve a high servo performance. In order to simulate the real resonance condition, the speed loop gain is high. T_f and T_{ci} can be calculated from an actual system. J_m can be obtained from the manufacture. J_L can be deduced by the motor speed response [26], the model reference adaptive system [27], [28], and by using a disturbance observer to identify the inertia [29], [30]. Then, K_s can calculate by the method in [22]. K_w can be calculated from the ratio between the open-loop gains at the resonant frequency of the motor under the no-load, rigidly-coupled load and compliantly-coupled load conditions.

When compared with the single bi-quad filter, the role of tuning A and B in the proposed double bi-quad filter is crucial. This can resolve the load side oscillation and affect the performance of the servo system. However, it is difficult to design A and B due to a high order of $G_L(s)$. The Pade Approximation is a common method to reduce the function order. Because the Pade Approximation has big effect on the high order part, the response characteristics of $G_L^*(s)$ ($G_L(s)$ by approximation) is very different from $G_L(s)$ at high frequencies. On the other hand, Pade Approximation has less effect on the low order part, so the response characteristic of $G_L^*(s)$ is similar to that of $G_L(s)$ on low and medium frequencies. Therefore, since resonance usually affects the response characteristics of servo systems at low and medium frequencies, the Pade Approximation can be used to reduce the order of $G_L(s)$. The original system can be reduced to a second-order system.

$$G_L^*(s) = \frac{KK_s}{M_1 s^2 + M_2 s + KK_s^2} \tag{10}$$

In which:

$$\begin{aligned} M_1 &= KK_w^2 + K_s^2\left(T_f + T_{ci}\right) - K_s^2 T_f \\ &\quad + BK_s - K_s K_w + KK_s^2 T_f^2 + AKK_s \\ &\quad - BKK_w - BKK_s T_f + KK_s K_w T_f \\ M_2 &= K_s^2 + BKK_s - KK_s K_w - KK_s^2 T_f \\ K &= \frac{K_n K_t}{J_m + J_L} \end{aligned} \tag{11}$$

Compared with a standard second-order system (Equ. (12)), Equ. (13) can be derived.

$$G(s) = \frac{\omega_n^2}{s^2 + 2\xi s + \omega_n^2} \tag{12}$$

TABLE I
EFFECT OF ΩN AND Ξ

ξ	ω_n	A/B	Load Side / Motor Side	
			Ts/s	Overshoot
0.3	100	0.141203 /7.6	0.1051 /0.1054	43.1% /43.4%
	200	0.032903 /3.1	0.0644 /0.0639	49.85% /51.4%
	400	0.006878 /0.85	0.04907 /0.05	61.75% /72.1%
	600	0.002369 /0.1	the convergence time is too long	
0.707	100	0.129807 /19.81	0.0283 /0.0281	4.45% /4.45%
	200	0.027205 /9.205	0.0137 /0.0134	4.48% /4.35%
	400	0.004029 /3.9025	0.0066 /0.0098	4.85% /6.20%
	700	-0.00016 /1.63	Divergent	
1.5	100	0.1076 /43.6	0.0817 /0.0819	0% /0%
	200	0.016103 /21.1	0.0411 /0.0409	0% /0%
	400	-0.00152 /9.85	Divergent	

$$\frac{KK_s^2}{M_1} = \omega_n^2, \quad \frac{M_2}{M_1} = 2\xi\omega_n \tag{13}$$

The expressions of A and B is shown as:

$$A = \frac{1}{K^2\omega_n^2}\begin{pmatrix} K^2K_s + K_s\omega_n^2 - KK_w\omega_n^2 \\ -KK_s\left(T_f + T_{ci}\right)\omega_n^2 \\ +2K^2K_w\omega_n\xi + K^2K_wT_f\omega_n^2 \\ -2KK_s\omega_n\xi + 2KK_sT_f\omega_n\xi \end{pmatrix} \tag{14a}$$

$$B = \frac{KK_w\omega_n - K_s\omega_n + 2KK_s\xi + KK_sT_f\omega_n}{K\omega_n} \tag{14b}$$

Simulations have been carried out and the results are displayed in Table I. In these simulations, K_n=500Hz, T_f=1ms, K_s=1500Nm/rad, K_w=0.1$Nm/(rad/s)$ and K_t=1.0Nm/A.

From Table I, it is found that ω_n and ξ have the same effect as an un-damped natural frequency and the damping ratio of a standard second-order system. When ξ is increased, the overshoot gets smaller. In addition, the speed loop response gets faster when ω_n increases. Table I may serve as a reference for the selection of ω_n and ξ. In general, ω_n and ξ decide the bandwidth of servo systems to some extent, and A, B are decided by ω_n and ξ. It should be noted that there is a mutual restriction between the speed loop response and the overshoot in the system. If both ξ and ω_n are designed too large, A and B will not be calculated correctly. As a result, the system will be unstable. In order to obtain a good performance, the selection of ω_n and ξ should make a compromise between the response and the overshoot.

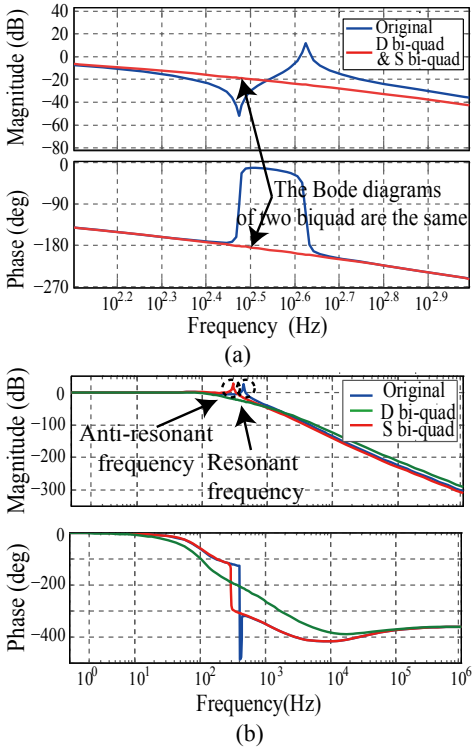

Fig. 10. (a) Motor side open-loop Bode diagram. (b) Load side Bode diagram.

C. Simulation Comparison

With the designed parameters, a performance comparison between the conventional single bi-quad filter and the proposed double bi-quad filter is carried out. For the simulation system, J_m is $1.0\times10^{-3}kg\cdot m^2$, J_L is $1.0\times10^{-3}kg\cdot m^2$, K_s is 3500Nm/rad, and K_w is 0.02$Nm/(rad/s)$.

In order to make a comprehensive consideration for the speed step response, the equivalent parameters are set as ω_n=600 and ξ=0.707, then A=0.00011502 and B=4.76833.

Motor side open loop Bode diagrams of three different conditions (without a filter, with a single bi-quad filter and with the proposed double bi-quad filter) are plotted in Fig. 10 (a). With the designed parameters, the motor side open-loop Bode plots with the single bi-quad filter and the proposed double bi-quad filter are the same. As a result, the comparison is fair. Furthermore, load side open-loop Bode diagrams without a filter, with a conventional single bi-quad filter and with the proposed double bi-quad filter are given in Fig. 10 (b). It can be found that on the motor side, the method with a single bi-quad filter and the proposed double bi-quad filter are both able to correct the system to a rigidly-coupled load and suppress resonance. However, on the load side, only the proposed double bi-quad filter can eliminate the gain peak at the anti-resonant frequency and suppress potential oscillations. With the single bi-quad filter, there exists a gain peak at the anti-resonant frequency which makes it easy for

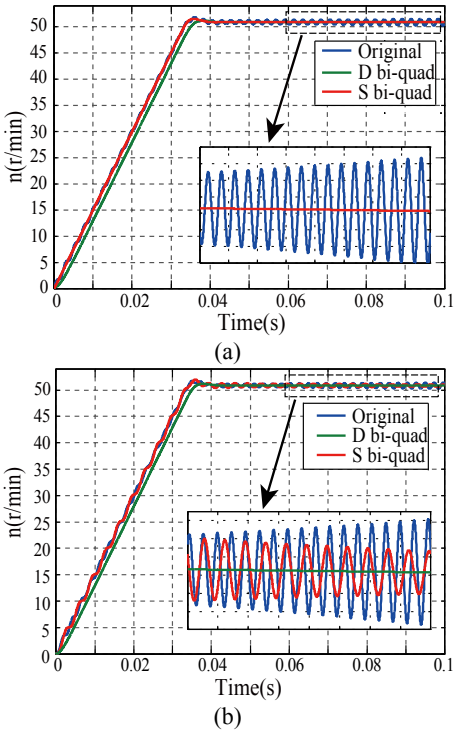

Fig. 11. (a) Motor side speed step response of two schemes. (b) Load side speed step response of two schemes.

oscillations to occur. These results can be verified by simulation waveforms of the speed loop step response as shown in Fig. 11.

IV. Analysis of Parameter Sensitivity

In the proposed double bi-quad filter, there are four parameters J_m, J_L, K_s and K_w decided by mechanical structures. Among them, J_m is a constant, but the parameter sensitivity of the others should be analyzed. In addition, the change of T_L needs to be investigated to determine whether it affects system stability.

A. Damping Constant K_w

In industry applications, the error of K_w comes from the parameter identification and the influence of the environment.

Fig. 12 shows a motor side open loop Bode plot without filters. It can be found that K_w mainly affects the peak in the amplitude near the resonant frequency and the anti-resonant frequency. However, the system's phase, resonant frequency and anti-resonant frequency do not deviate. The simulation result shows a change of K_w does not have a large influence on the resonance suppression of the double bi-quad filter.

In fact, the damping constant K_w has so little effect on the performance of a servo system so that many scholars ignore it in the analysis of resonance problems.

B. Spring Constant K_s and Load Inertia J_L

Changes of K_s and J_L cause the deviation of the resonant frequency and the anti-resonant frequency, and have a bigger

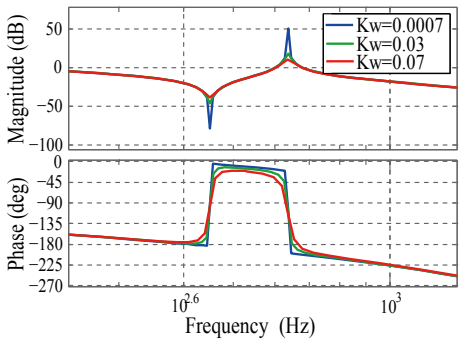

Fig. 12. Under different conditions, Bode plots of G2(s). In which, K_s=3000Nm/rad, J_m=J_L=1.0×10^{-3}$kg{\cdot}m^2$.

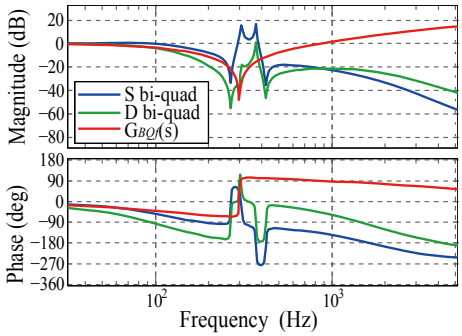

Fig. 13. Bode plot of $1/G_{BQf}(s)$ and Bode plot of two schemes from ω_{ref} to ω_m.

influence on systems. The parameter sensitivity analysis of K_s and J_L should be divided into two parts: 1) the changes of K_s and J_L that reduce the stability margin, while the system remains stable; 2) the changes of K_s and J_L that make the system unstable.

In the first case, on the motor side, the double bi-quad filter is equivalent to adding a filter $1/G_{BQf}(s)$ on the motor speed output side. Fig. 13 shows a Bode plot of $1/G_{BQf}(s)$ and two schemes from ω_{ref} to ω_m. It can be seen that $1/G_{BQf}(s)$ can reduce gains near the resonance frequency, and smooth the motor speed.

Consequently, the motor steady state speed of the proposed double bi-quad filter is more stable than the single bi-quad filter, when changes of K_s and J_L only cause a reduction in the stability margin, as shown in Fig. 14 and Fig. 15.

In the second case, the closed loop system is unstable on the motor side. $1/G_{BQf}(s)$ does not work anymore. Therefore, parameter modification and reconstruction are necessary for the double bi-quad filter. Reconstruction schemes can be classified into two different branches as follows:

1) Slight Change of K_s: The K_s of some connecter parts such as solid coupling, gears and reduction boxes cannot change if the mechanical lifetime is very long and plastic deformation does not occur.

In addition, by using the proposed method, the accuracy of the K_s measurement is pretty high (if the error of f_{res} is very small, and the off-line measurement of J_L is constant). In this situation, K_s can be treated as a constant, and the system

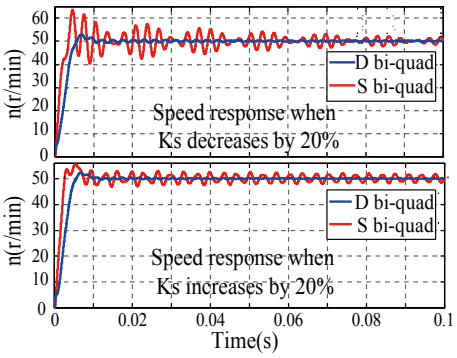

(a)

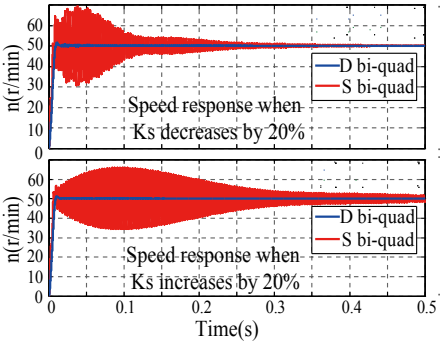

(b)

Fig. 14. When system is stable, K_s is changed 20%. (a) Speed step response on motor side. (b) Speed step response on load side.

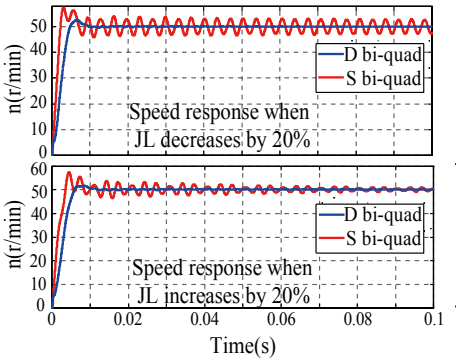

(a)

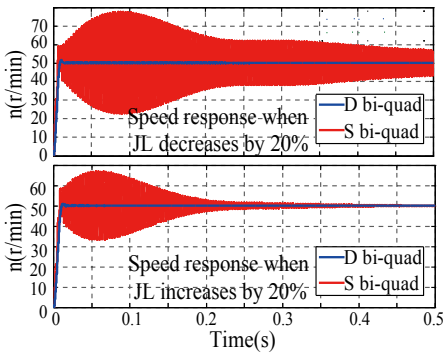

(b)

Fig. 15. When system is stable, J_L is change 20%. (a) Speed step response on motor side. (b) Speed step response on load side.

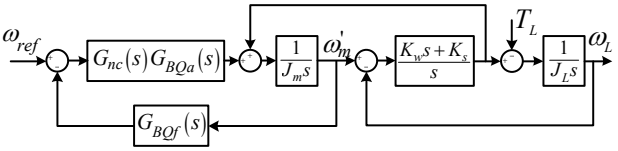

Fig. 16. double bi-quad filter system with T_L.

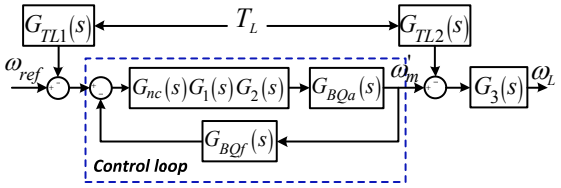

Fig. 17. Transformed system from Fig. 16.

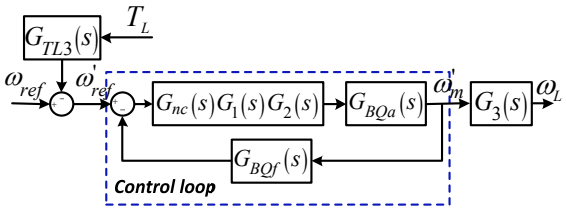

Fig. 18. Transform T_L effect to input side.

resonance frequency changes mainly due to changes of J_L.

Under this kind of circumstance, when system resonance reoccurs, J_L can be recalculated by online measurement of the resonance peak frequency f_{res}. With the updated J_L, the proposed double bi-quad filter is reconstructed, and can be used to replace former double bi-quad filter.

2) Slight Change of J_L: The J_L of some equipment does not change frequently, such as laser phototypesetters, laser engraving machines, etc. For these cases, J_L can be treated as a constant to solve the resonance problem. A change of K_s should be considered as the main cause of f_{res} modification. When system resonance reoccurs, K_s can be recalculated by online measurement of the resonance peak frequency f_{res}.

C. Load Torque T_L

When studying compliant coupling, T_L is generally neglected. If the effects of T_L are considered, Fig. 9 becomes more complicated, as shown in Fig. 16.

Fig. 16 can be transformed as Fig.17.

In Fig. 17:

$$G_{TL1}(s) = \frac{G_3(s)}{G_{nc}(s)} \tag{15}$$

$$G_{TL2}(s) = \frac{s}{K_w s + K_s} \tag{16}$$

Finally, the effect of T_L can be transformed to the input side, which is shown in Fig. 18.

In Fig. 18:

$$G_{TL3}(s) = G_{TL1}(s) + \frac{G_{TL2}(s)}{G_B(s)} \tag{17}$$

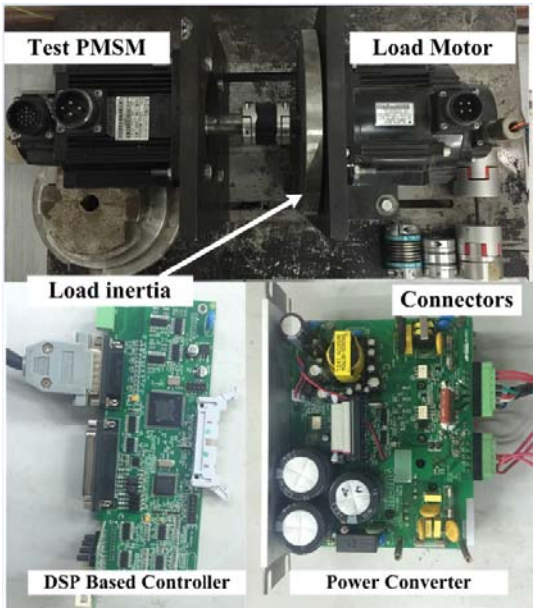

Fig. 19. Experimental setup used to test proposed methods.

TABLE II

XGT2-44C'S PARAMETERS

Parameter	XGT2-44C
K_s	1300*Nm/rad*
Inertia	$4.1\times10^{-5}kg{\cdot}m^2$
Rated torque	18*N.m*

$G_B(s)$ is the transfer function from ω_{ref}' to ω_m'.

When compared with Fig. 9, the effect of T_L is equivalent to adding an extra speed reference at the input side, and it has no effects on the system closed-loop characteristics. Thus, the proposed double bi-quad need not be reconstructed regardless of whether T_L changes or not. In [25], the experimental results have verified that changes of the load torque have no effect on the filter suppression methods. Therefore, most of the experiments in previously published papers are implemented under no the load condition [19], [32], [33].

V. EXPERIMENTAL RESULTS

In this section, several experiments have been implemented to validate the proposed double bi-quad filter. The system setup for experimental testing is shown in Fig. 19. The control algorithm is implemented through a TI TMS320F28035 DSP. The specifications and parameters of the testing PMSM are listed as follows: the rated power is 1.3*KW*, rated speed is 2500*rpm*, rated current is 5*A*, torque coefficient is 1.0*N.m/A*, and rotor inertia is $1.03\times10^{-3}kg{\cdot}m^2$. A Yaskawa SGMGV 13ADC61 motor acts as the load. Its rated power is 1.3*KW*, rated speed is 1500*rpm*, rated current is 10.7*A*, torque coefficient is 0.89*N.m/A*, and rotor inertia is $1.99\times10^{-3}kg{\cdot}m^2$. Metal plates can be added to simulate load inertia.

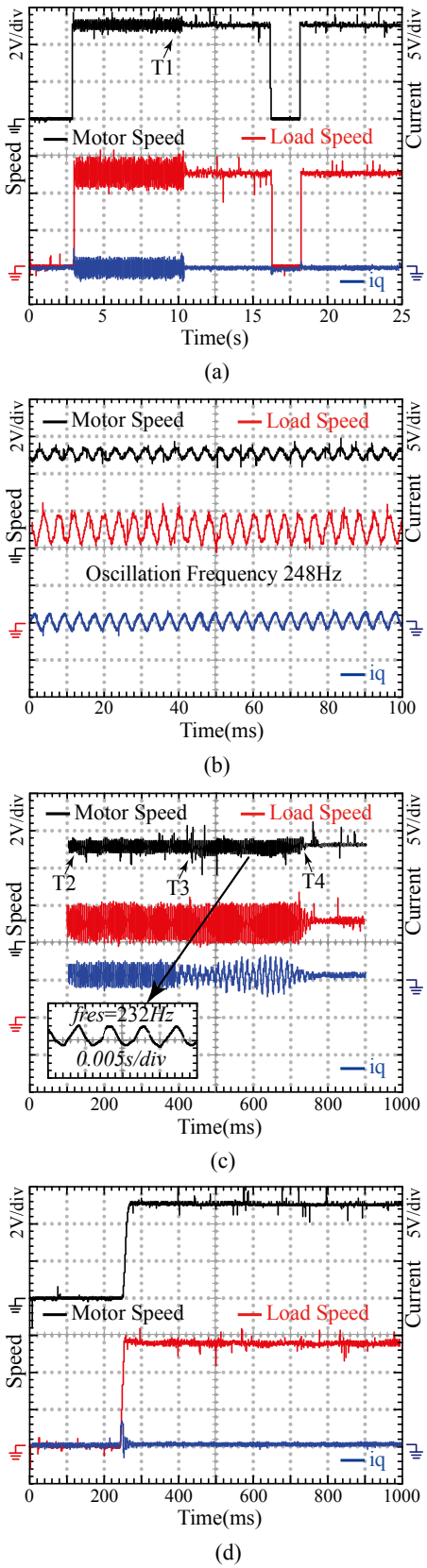

Fig. 20. (a) Whole resonance suppressing process. (b) A partial view of oscillation without suppression. (c) Automatically resonance suppression. (d) Speed increase after adding double bi-quad filter.

The motor speed is output by the experimental servo's DA module, and the load's speed is output by the Yaskawa's DA module. In the oscilloscope, $1V$ represents $30rpm$ and $1A$, respectively. The delay times T_f and T_{ci} are calculated as $1ms$ and $33us$, respectively. K_n is set as $450Hz$. According to Section IV, Part C, the magnitude of load torque has no effects on the double bi-quad filter. Thus, for ease of operation, all of the experiments are implemented under the no load condition.

A. High-frequency Resonance Experiment

The high-frequency resonance performance and system performance with the proposed double bi-quad filter is verified in this sub-section. A NBK's XGT2-44C is used as the connected part and its specific parameters are shown in Table II. The mechanical damping constant $K_w \approx 0.11Nm/(rad/s)$.

Fig. 20(a) shows the whole process of resonance suppression when the load inertia does not increase. With a step reference of $150rpm$, the system oscillates with a frequency of $248Hz$, as shown in Fig. 20(b). Then, the system automatically starts resonance suppression at time T1 as shown in Fig. 20(a). This process is divided into two stages.

1) Adding the first and second low pass filter at time T2 and T3, respectively. The frequency f_{res} can be identified as $232Hz$ by the change in the speed oscillation amplitude. K_s is calculated as $1412Nm.rad$, as shown in Fig. 20(c).
2) According to Table I, comprehensively consider the speed loop response, overshoot and system stability, while setting ω_n=400 and ξ=0.707. Calculate A=0.005363, B=4.3837 from Equ. (14). The proposed Double bi-quad filter is built and then added to the system at time T4. Finally complete the resonance suppression as shown in Fig. 20(a) and (c).

Fig. 20(d) shows that by adding the double bi-quad filter, the waveform's speed increases. The waveform shows that the proposed double bi-quad filter achieves the desired goal since the resonance on both the motor and load sides are suppressed.

In order to simulate load inertia variations, a metal plate (its inertia is $0.01kg{\cdot}m^2$) is added on the load side, and f_{res} is changed. The original double bi-quad filter suppressing effect cannot be achieved. Therefore, the filter needs to be reconstructed. The whole process is shown in Fig. 21(a).

At T5, the original double bi-quad filter is added, but the system still oscillates. At T6, the original double bi-quad filter is removed. At T7, the system starts to reconstruct the double bi-quad filter.

Fig. 21(b) shows that the speed oscillation frequency is changed to $224Hz$. Fig. 21(c) shows the details of reconstruction process. At T8 and T9, the first and second low-pass filter are added resulting in f_{res}=196Hz. According to the principle that K_s does not change, the calculated new

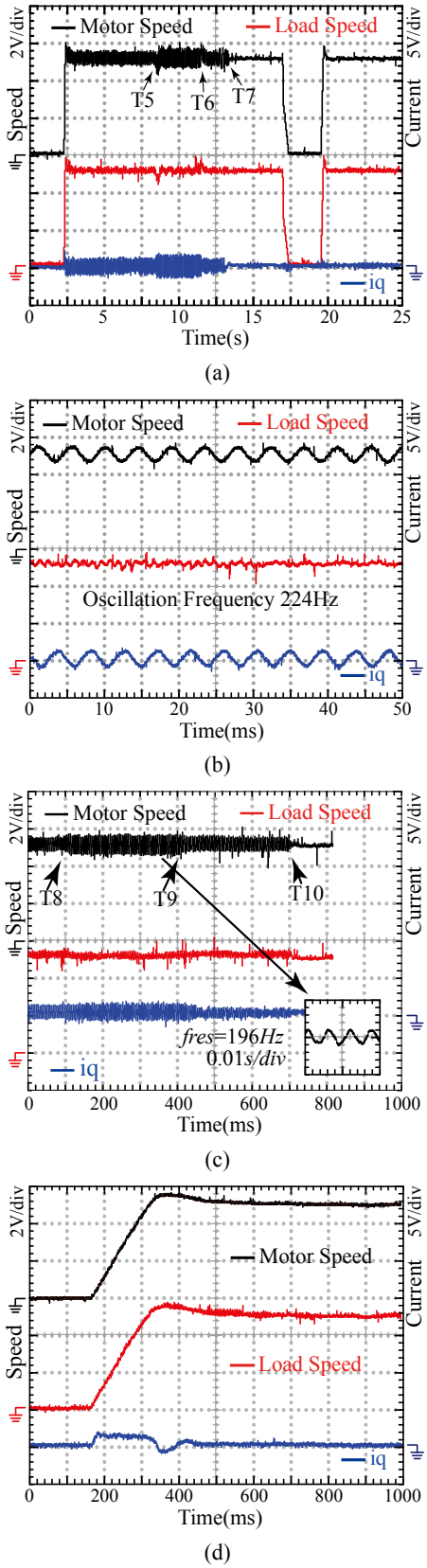

Fig. 21. (a) Whole resonance suppressing process. (b) A partial view of oscillation without suppression. (c) Reconstruct a new double bi-quad filter. (d) Speed increase after adding new double bi-quad filter.

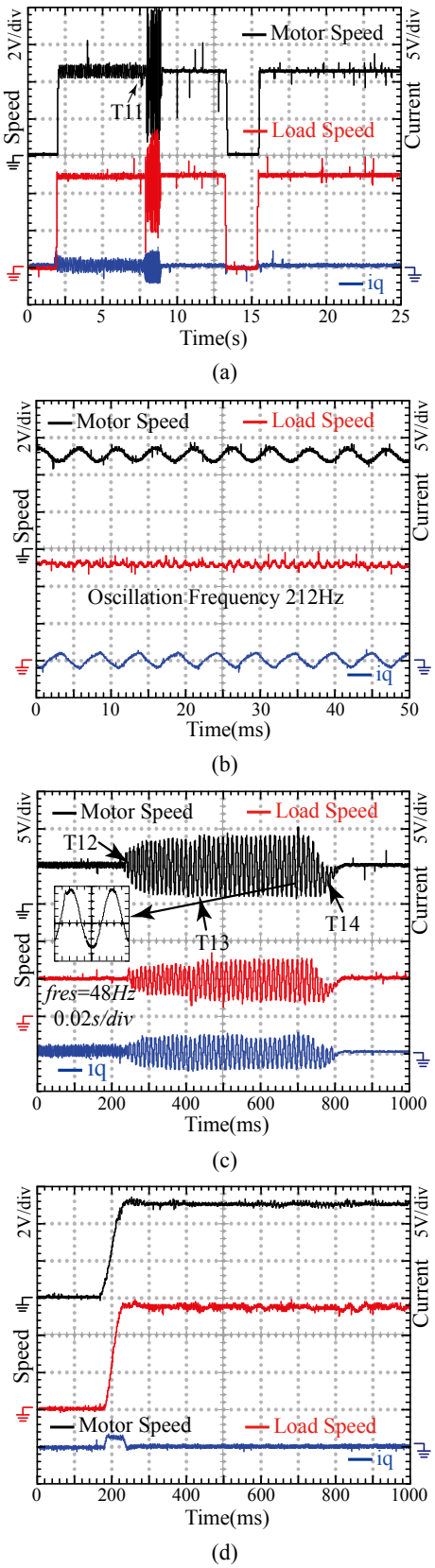

Fig. 22. (a) Whole resonance suppressing process for low-frequency. (b) A partial view of oscillation without suppression. (c) Automatically resonance suppression. (d) Speed increase after adding double bi-quad filter.

load inertia is 0.0137 $kg{\cdot}m^2$, where A=0.0029606 and B=2.00223. At T10, a new filter is reconstructed and the resonance suppression is complete.

Fig. 21 (d) shows the details of the system speed increase. Fig. 21 shows that the double bi-quad filter can be achieved by online reconstruction to offset the system parameter changes.

B. Low-frequency Resonance Experiment

During the second experiment, a self-made low K_s coupling is used as the connector. Its aim is to verify the effect of the double bi-quad filter suppression for low-frequency resonance. The coupling's damping constant is 0.1 *Nm*/(*rad*/*s*). It is noted that since the spring constant is low, the load side does not oscillate much.

Fig. 22(a) shows the whole process of the low-frequency resonance, in which the adaptive procedure starts at T11. Fig. 22(b) shows that the oscillation frequency is 212*Hz*. Fig. 22(c) shows the process of automatic resonance suppression, where two low pass filter are added at T12 and T13. This results in f_{res}≈48*Hz* and K_s≈60.4*Nm.rad*. Set ω_n=400 and ξ=0.707, and tune A=0.0002543 and B=0.18094. Finally, the double bi-quad filter is constructed at T14, and the resonance suppression is complete. Fig. 22(d) shows the details of the system speed up.

Fig. 22 shows the experiment reaching its intended goal since the proposed double bi-quad filter for low-frequency resonance has a good suppression of resonance oscillations. Since K_s is small, the effect of J_L changing is not obvious. As a result, there are no further reconstruction experiments.

VI. Conclusion

When compared with a single bi-quad filter, the proposed double bi-quad filter method is actually equivalent to add a virtual filter after the motor speed output. It contains two bi-quad filters on both the forward and feedback paths of the speed control loop. The two filters collectively complete the wide-band resonance suppression, and the filter on the feedback path can solve the problem of oscillation on the load side. Meanwhile, if the stability margin is reduced by parameter errors, but the system is still stable, the proposed structure can alleviate the damage caused by parameter errors. Simulation and experimental results confirm the validity of the theoretical conclusions and the advantageous performance of the improved control algorithm.

References

[1] W. L. Zhao, T. A. Lipo, and B.-I. Kwon, "Material-efficient permanent-magnet shape for torque pulsation minimization in SPM motors for automotive applications," *IEEE Trans. Ind. Electron.*, Vol. 61, No. 10, pp.5779-5787, Oct. 2014.

[2] X. D. Li and S. H. Li, "Speed control for a PMSM servo system using model reference adaptive control and an

extended state observer," *Journal of Power Electronics*, Vol. 14, No. 3, pp. 549-563, May 2014.
[3] J. Na, Q. Chen, X. M. Ren, and Y. Guo, "Adaptive prescribed performance motion control of servo mechanisms with friction compensation," *IEEE Trans. Ind. Electron.*, Vol. 61, No. 1, pp. 486-494, Jan. 2014.
[4] O.-S. Park, J.-W. Park, C.-B. Bae, and J.-M. Kim "A dead time compensation algorithm of independent multi-phase PMSM with three-dimensional space vector control," *Journal of Power Electronics*, Vol. 13, No. 1, pp. 77-85, Jan. 2013.
[5] M. T. Elsayed, O. A. Mahgoub, and S. A. Zaid, "Simulation study of a new approach for field weakening control of PMSM," *Journal of Power Electronics*, Vol. 12, No. 1, pp. 136,144, Jan. 2012.
[6] H. H. Choi, N. T.-T. Vu, and J.-W. Jung, "Design and implementation of a Takagi–Sugeno fuzzy speed regulator for a permanent magnet synchronous motor," *IEEE Trans. Ind. Electron.*, Vol. 59, No. 8, pp. 3069-3077, Aug. 2012.
[7] D. Torregrossa, A. Khoobroo, and B. Fahimi, "Prediction of acoustic noise and torque pulsation in PM synchronous machines with static eccentricity and partial demagnetization using field reconstruction method," *IEEE Trans. Ind. Electron.*, Vol. 59, No. 2, pp. 934-944, Feb. 2012.
[8] G. Zhang, "Speed control of two-inertia system by PI/PID control," *IEEE Trans. Ind. Electron.*, Vol. 47, No. 3, pp. 603-609, Jun. 2000.
[9] M.-C. Pera, D. Candusso, D. Hissel, and J. M. Kauffmann, "Enhanced servo-control performance of dual-mass systems," *IEEE Trans. Ind. Electron.*, Vol. 54, No. 3, pp. 1387-1399, Jun. 2007.
[10] S. N. Vukosavic and M. R. Stojic, "Suppression of torsional oscillations in a high-performance speed servo drive," *IEEE Trans. Ind. Electron.*, Vol. 45, No. 1, pp. 108-117, Feb. 1998.
[11] K. Itoh, M. Iwasaki, and N. Matsui, "Optimal design of robust vibration suppression controller using genetic algorithms," *IEEE Trans. Ind. Electron.*, Vol. 51, No. 5, pp. 947-953, Oct. 2004.
[12] K. Ito and M. Iwasaki, "GA-based practical compensator design for a motion control system," *IEEE/ASME Trans. Mechatron.,* Vol. 6, No. 2, pp. 143-148, Jun. 2001.
[13] G. Ellis and R. D. Lorenz, "Resonant load control methods for industrial servo drives," in *Proc. IAS*, pp. 1438-1445, 2000.
[14] K. Sugiura and Y. Hori, "Vibration suppression in 2- and 3-mass system based on the feedback of imperfect derivative of the estimated torsional torque," *IEEE Trans. Ind. Electron.*, Vol. 43, No. 1, pp. 56-64, Feb. 1996.
[15] G. Ellis and Z. Q. Gao, "Cures for low-frequency mechanical resonance in industrial servo systems," in *Proc. IAS*, pp. 252-258, 2001.
[16] K. Szabat and T. Orlowska-Kowalska, "Vibration suppression in a two-mass drive system using PI speed controller and additional feedbacks—comparative study," *IEEE Trans. Ind. Electron.*, Vol. 54, No. 2, pp. 1193-1206, Apr. 2007.
[17] V. P. Makkapati, M. Reichhartinger, and M. Horn, "Performance improvement of servo drives with mechanical elasticity via Extended Acceleration Feedback," in *Proc. CCA*, pp. 1279-1284, 2012.
[18] P. Schmidt and T. Rehm, "Notch filter tuning for resonant frequency reduction in dual inertia systems," in *Proc. IAS*, pp. 1730-1734, 1999.
[19] M. A. Valenzuela, J. M. Bentley, A. Villablanca, and R. D. Lorenz, "Dynamic compensation of torsional oscillation in paper machine sections," *IEEE Trans. Ind. Appl.*, Vol. 41, No. 6, pp. 1458-1466, Nov./Dec. 2005.
[20] J. Kang, S. L. Chen, and X. G. Di, "Online detection and suppression of mechanical resonance for servo system," in *Proc. ICICP*, pp. 16-21, 2012.
[21] P. Liu, D. B. Zhao, L. Zhang, and W. Zhang, "Design of notch filter applied in miniaturized NC micro-milling machine tool," in *Proc. IEEE Knowledge Acquisition and Modeling Workshop,* pp. 928-931, 2008.
[22] W. Y. Wang, J. B. Xu, and A. W. Shen, "Detection and reduction of middle frequency resonance for industrial servo," in *Proc. ICICP,* pp. 153-160, 2012.
[23] T. Orlowska-Kowalska and K. Szabat, "Damping of torsional vibrations in two-mass system using adaptive sliding neuro-fuzzy approach," *IEEE Trans. Ind. Informat.*, Vol. 4, No. 1, pp. 47-57, Feb. 2008.
[24] T. Orlowska-Kowalska, M. Dybkowski, "Stator current based MRAS estimator for a wide range speed-sensorless induction-motor drive," *IEEE Trans. Ind. Electron.*, Vol. 57, No. 4, pp. 1296-1308, Apr. 2010.
[25] S. Brock and D. Luczak, "Speed control in direct drive with non-stiff load," in *Proc. ISIE*, pp. 1937-1942, 2011
[26] B. Zhang, Y. H. Li, and Y. S. Zuo, "A DSP-based fully digital PMSM servo drive using on-line self-tuning PI controller," in *Proc. IPEMC*, pp. 1012-1017, 2000.
[27] L. Guo and W. H. Chen, "Disturbance attenuation and rejection for a class of nonlinear systems via DOBC approach," *Int. J. Robust Nonlinear Control*, Vol. 15, No. 3, pp. 109-125, Feb. 2005.
[28] Y. J Guo, L. P. Huang, Y. Qiu, and M. Maramatsu, "Inertia identification and auto-tuning of induction motor using MRAS," in *Proc. IPEMC*, pp. 1006-1011, 2000.
[29] R. Garrido and A. Concha, "Inertia and Friction estimation of a velocity-controlled servo using position measurements," *IEEE Trans. Ind. Electron.*, Vol. 61, No. 9, pp .4759-4770, Sep. 2014.
[30] S. M. Yang amd Y. J. Deng, "Observer-based inertial identification for auto-tuning servo motor drives," in *Proc. IAS*, pp. 968-972, 2005.
[31] L. Harnefors and N. Hans-Peter, "Model-based current control of AC machines using the internal model control method," *IEEE Trans. Ind. Appl.*, Vol. 34, No. 1, pp. 133-141, Jan./Feb. 1998.
[32] D. H. Lee, J. H. Lee, and J. W. Ahn "Mechanical vibration reduction control of two-masspermanent magnet synchronous motor using adaptivenotch filter with fast Fourier transform analysis," *IET Electric Power Appl.*, Vol. 6, No. 7, pp. 455-461, Aug. 2012.
[33] H. J. Wang, D. H. Lee, Z. G. Lee, and J. W. Ahn, "Vibration rejection scheme of servo drive system with adaptive notch filter," in *Proc. PESC*, pp. 1-6, Jun. 2006.

Xin Luo received his B.S. and M.S. degrees from the Huazhong University of Science and Technology, Hubei, China, in 2007 and 2010, respectively, where he is presently working towards his Ph.D. degree. His current research interests include PMSM drive systems and power conversion circuits.

Anwen Shen received his B.S. and M.S. degrees from Zhejiang University, Zhejiang, China, in 1991 and 1994, respectively, and his Ph.D. degree in Electric Drives and Automation from the Department of Control Science and Engineering, Huazhong University of Science and Technology (HUST), Wuhan, China, in 1997. He is presently a Professor in the School of Automation, HUST. His current research interests include power electronics, electrical drives, and intelligent control.

Renchao Mao received his B.S. degree in Automation from the Department of Control Science and Engineering, Huazhong University of Science and Technology (HUST), Wuhan, China, in 2012, where he is presently working toward his M.S. degree in Control Science and Engineering. His current research interests include power electronics and motion control.